Surface Energy and Water Balance for the Arkansas–Red River Basin from the ECMWF Reanalysis

ALAN K. BETTS

Pittsford, Vermont

PEDRO VITERBO

ECMWF, Reading, Berkshire, United Kingdom

ERIC WOOD

Water Resources Program, Princeton University, Princeton, New Jersey

(Manuscript received 28 October 1997, in final form 3 February 1998)

ABSTRACT

Average surface energy and water budgets, subsurface variables, and atmospheric profiles were computed online with an hourly timescale from the ECMWF reanalysis for five subbasins of the Mississippi River from 1985–93. The results for the Arkansas–Red River basin are discussed on diurnal, 5-day, monthly, seasonal, and interannual timescales, and compared with the observed basin-scale precipitation and streamflow. The model shows the seasonal and interannual variability of precipitation, evaporation, and soil water. The annual range of soil water is typically 100 mm, and the interannual range is somewhat smaller. The model has a significant spinup of about 29% in precipitation from the analysis cycle to a 12–24-h forecast. The spinup of the model ''large-scale'' precipitation is 39%, double that of the spinup of the model ''convective'' precipitation of 18%. When compared with 5-day and monthly basin averages of hourly rain gauge observations (corrected for a probable 10% low bias), the precipitation in the reanalysis is low by 20%–25%, while the 12–24-h forecast precipitation is high by about 5%; so the model precipitation estimates the bracket observations. The nudging of soil water in the analysis cycle, based on 0–6-h forecast errors in low-level humidity, plays an important role in the model liquid hydrology. It prevents the downward interannual drift of soil water, associated with a shortfall of precipitation in the analysis cycle, while allowing interannual variations of soil water. However, the nudging appears to be trying to compensate for other errors in the model: such as errors in the diurnal cycle of low-level mixing ratio and in the seasonal cycle of evaporation. Evaporation in the model is probably high in winter, and on an annual basis may have a small high bias in comparison to a basin evaporation estimate derived from observed precipitation and streamflow. An internal inconsistency of 7% in the evaporation term in the model surface energy and subsurface water budgets is also found, dating from an earlier model version. The coupling of soil water in the model to evaporative fraction and the low-level thermodynamics is similar to that observed. The model runoff, which is all deep runoff from the base soil layer, is low by a factor of 2, when compared to observed streamflow on an annual basis. The model diurnal cycle of precipitation has a near-noon maximum, while that observed is late afternoon and evening. This is probably related to the model error in the diurnal cycle of mixing ratio and boundary layer depth. Overall the ECMWF reanalysis gives a valuable description of the surface energy and water balance of the Arkansas–Red River basin on timescales longer than the diurnal.

1. Introduction

A key objective of the Global Energy and Water Experiment Continental International Project (GCIP) was to assess the ability of our forecast models to estimate the energy and hydrological balances on river basin scales, and to use observations of precipitation and runoff as evaluation data. By improving the surface evaporation and hydrological response of our forecast models, improvements can be made in medium-range to seasonal-scale prediction (Beljaars et al. 1996). The European Centre for Medium-Range Weather Forecasts (ECMWF) recently completed its reanalysis project, which used a frozen version of their analysis–forecast system, at a triangular spectral truncation of T-106 with 31 levels in the vertical, to perform data assimilation using past data from 1979 to 1993 (Gibson et al. 1997). The study of climate and climate change is driving the need for these uniformly assimilated datasets. The pre-

Corresponding author address: Dr. Alan K. Betts, 58 Hendee Ln., Pittsford, VT 05763.
E-mail: akbetts@aol.com

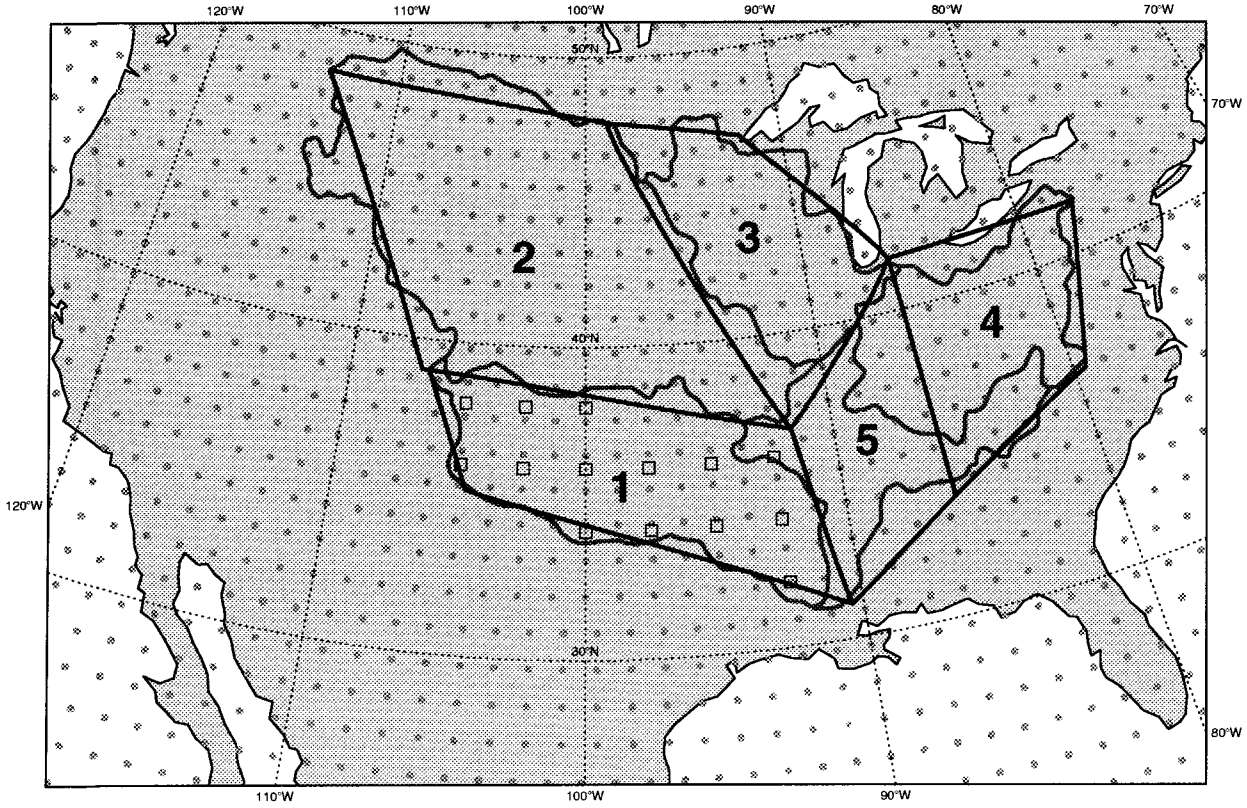

FIG. 1. U.S. section of ECMWF model, showing physics grid points (shaded dots), together with outlines of five major Mississippi subbasins, and their approximation in the EC model by quadrilaterals. Small squares are data points for Higgins et al. (1996) gridded rainfall set.

vious archives of gridpoint data were derived from operational numerical weather prediction centers, and were the results of production data assimilation suites. In studies of the climate change to date, researchers have had to deal with changes in the model data due both to real atmospheric changes and due to changes in assimilation procedures. For this reason reanalysis projects were proposed some years ago (Bengtsson and Shukla 1988) to remove changes due to assimilation procedures as much as possible. The ECMWF reanalysis has a 6-h analysis cycle, and from every analysis a 6-h short-term forecast is run. The meteorological state variables at the surface are archived at 3 and 6 h from these forecasts, as well as the surface fluxes averaged for the 0–3- and 3–6-h forecasts. However, in addition to this 3-h gridpoint archive, certain grid points and averaged quadrilaterals of grid points were archived at an hourly time resolution. One set of averages were for the five main subbasins of the Mississippi from 1985–93. This online domain integration capability is a unique aspect of the ECMWF data assimilation system. Figure 1 shows the physics grid points (as dots) of the ECMWF T-106 reanalysis model for the United States: superimposed are the outlines of the five major Mississippi subbasins and their approximation in the reanalysis model by quadrilaterals. In clockwise sequence, basin 1 comprises the Arkansas–Red Rivers, basin 2 the upper Missouri, basin 3 the upper Mississippi, basin 4 the Ohio, and 5 the lower Mississippi and Tennessee Rivers (rather more poorly represented than the others). Table 1 shows the drainage area of the five basins from Seaber et al. (1987) and the corresponding model area.

TABLE 1. Mississippi subbasin drainage areas and their model approximation.

Subbasin	Drainage area (km^2)	Model area (km^2)
1	636 400	677 700
2	1 320 800	1 285 700
3	490 200	567 700
4	418 000	351 400
5	299 100	390 500

Understanding how well we can model the seasonal and interannual variation of the surface energy and hydrological balances of the Mississippi subbasins is a key objective of GCIP. To this end, an archive has been compiled of averages (as single-column datasets) for these five Mississippi subbasins, both from the ECMWF reanalysis (for 1985–93), and an ongoing archive from 1996 from the current T-213 operational model.

In this paper we analyze the hydrologic and energetic

budgets for the Arkansas–Red River subbasin of the Mississippi (basin 1) for this 9-yr period 1985–93. We look at the diurnal, 5-day, monthly, seasonal, and interannual variability of precipitation, soil water, surface evaporation, and runoff in the model, as well as the surface energy budget. We shall also discuss the links between soil water, evaporative fraction, and boundary layer thermodynamics on the scale of this basin.

2. Model and observed datasets

a. The ECMWF reanalysis model

The hourly basin average archive includes both the short-term forecasts (hourly to 6 h) used in the reanalysis cycle, and twice-daily 24-h forecasts from 0000 and 1200 UTC (archived hourly), so that issues relating to the diurnal cycle and the spinup in the precipitation field can be addressed. We shall show model precipitation for the same verifying times from both the 0–6-h analysis cycle (this we shall refer to as analysis precipitation), and from the 12–24-h sections of the twice-daily 24-h forecasts (which we shall refer to as 12–24-FX precipitation). The model has a significant initial spinup of precipitation from the analysis to the 12–24-h forecast, and we shall find that the observed precipitation lies between these two model estimates.

Model precipitation is subdivided into convective and large-scale rain, and convective and large-scale snowfall. Convective snowfall is negligible for this basin and large-scale snowfall is small. The ECMWF reanalysis model handles liquid and solid precipitation differently, and our analysis will be primarily concerned with the liquid phase, which refills the soil reservoir (and also runs off). The frozen phase is treated as a snow layer on the surface (Viterbo and Beljaars 1995), which can melt or evaporate to the atmosphere, but its hydrology is not conservative, since an independent snow analysis is introduced at every analysis time. For this Red–Arkansas basin, fortunately, the percent of precipitation that falls as snow is only 3% on an annual basis, and snowmelt is a still smaller term (<0.5% of rainfall). When comparing with observations, which are total precipitation (although they underestimate snowfall more than rain), we shall show total model precipitation; but when discussing the model liquid hydrology, we shall show model rainfall.

A recent study of the ECMWF reanalysis model (Betts et al. 1998) used average data from the First International Satellite Land Surface Climatology Project Field Experiment (FIFE) for the summer season of 1987 to assess the land surface interaction of the ECMWF reanalysis at a single grid point. In comparison with a previous study (Betts et al. 1993), they found the land surface interaction to be greatly improved. The bias in the incoming solar radiation is now small. The four-layer soil water model (Viterbo and Beljaars 1995) depicts the seasonal cycle well, and the root zone is recharged satisfactorily after major rain events. Consequently, the evaporative fraction (EF) over the season for this grassland location in Kansas is now generally quite good. In comparison with the data, however, the model has a low bias in EF in June and a high bias in October, which is probably due to the absence of a seasonal cycle in the model vegetation. The EF also appears too high in the model just after rainfall. In addition, the surface diurnal thermodynamic cycle has two noticeable errors. The temperature minimum at sunrise is too low, because the surface uncouples and cools too much at night under the stable boundary layer (BL), and the incoming longwave radiation at night is biased low. There is also an unrealistic diurnal cycle of mixing ratio, q, with too strong a midmorning peak, and too large a fall during the day to a late afternoon minimum that is biased low. The morning peak is partly related to the too-strong inversion at sunrise, which slows the deepening of the BL. Betts et al. (1998) found that the ECMWF reanalysis appears to have errors in the diurnal cycle of precipitation. There is a mid-to-late morning peak in precipitation, which may be related to a midmorning peak in mixing ratio (which is also seen in equivalent potential temperature, θ_E), or to the convection scheme. This study will confirm that this diurnal precipitation error exists on the basin scale.

In the reanalysis model, however, some of the improvements in evaporation came from adding soil water nudging to the analysis cycle, based on the q analysis increment in the short term 0–6-h forecast for the lowest model level mixing ratio. This is a small but significant component in the subsurface hydrological budget. The total addition of soil water to the top three layers (the root zone of 1-m depth) in a 6-h analysis interval (Δt) is calculated from

$$\Delta(\mathrm{SW}) = C_v D \Delta t (q_a - q_g), \qquad (1)$$

where C_v is the vegetation fraction (included so that there is no nudging over deserts). In the reanalysis model, the coefficient D is set so that, if the moisture analysis increment $(q_a - q_g) = 3$ g Kg^{-1}, then 0.15 m of water is added to the soil in 12 days (the operational model uses a higher rate of nudging; the corresponding timescale is 4.5 days). Normally the nudging is applied uniformly to the first three layers in the 1-m root zone (0–7, 7–28, and 28–100 cm), but there is, in addition, a constraint for each individual layer that the field capacity and the permanent wilting point thresholds are never crossed by the nudging. In our hourly dataset, the nudging increments were not explicitly stored, so we had to recalculate them from the change in soil water at analysis times. There are a few missing analysis times in our hourly dataset (when the archiving failed), where we cannot recompute the nudging and must substitute some appropriate mean value.

From the seasonal hydrology at the FIFE site for 1987, Betts et al. (1998) suggested that the nudging increment may be compensating for a spinup in precip-

itation, but may also be producing slightly high evaporation. They also noticed that the late afternoon minimum of mixing ratio (below that of the model analysis) leads to a positive nudging of soil water in the analysis cycle, and speculated that some of this feedback between errors in the model diurnal cycle of water and the nudging might be spurious. On the basin scale we shall find that it appears that the nudging is compensating not only for the spinup of precipitation, but also for seasonal errors in evaporation.

b. Validation data

We have two sets of validation data. One is the Higgins et al. (1996) hourly gridded precipitation dataset, from which we extracted the data for 1985–93, and calculated a simple basin average from the $2^\circ \times 2.5^\circ$ data, using the 14 grid points that have centers within the ECMWF averaging quadrilateral, shown as small squares in Fig. 1. Gauge estimates of precipitation tend to be underestimates (Groisman and Legates 1994). The hourly precipitation data is mostly from Fisher and Porter gauges, which Groisman (1997, personal communication) estimates to have a 10% low bias for rainfall, and a larger low bias for snowfall. In this paper we are primarily concerned with the liquid hydrology, so we assign a nominal 10% low bias to this precipitation data.

The second is basin-averaged data, aggregated from the dataset of Wood et al. (1998) consisting of daily and hourly precipitation data from 1985–88, and observed streamflow data for the basin from 1985–90. The precipitation dataset was part of an hourly, 10-yr atmospheric forcing dataset for 1979–88, appropriate for land surface modeling, which is described in Wood et al. (1998). Only the years 1985–88 of the precipitation data are used here. Daily precipitation data were assembled by Abdulla et al. (1996) from National Oceanographic and Atmospheric Administration/National Climate Data Center (NOAA/NCDC) cooperator stations and aggregated to $1^\circ \times 1^\circ$ grids by simple averaging. In most cases, there were two precipitation stations per grid cell. Daily precipitation was then adjusted to an hourly time step and the fractional precipitation coverage (of the $1^\circ \times 1^\circ$ grids) estimated by making use of hourly manually digitized radar (MDR) data. The MDR data were used only to provide the hourly rainfall pattern, the relative hourly depths, and the rainfall fractional coverage for the grids. The daily totals were then temporally distributed on this basis and adjusted for fractional coverage so as to maintain the NOAA/NCDC gauge-based, grid total precipitation. In this analysis we shall only present 9-yr averages of the diurnal cycle of precipitation, based on the Higgins et al. dataset, as these are sufficient to show that the reanalysis model has a large diurnal error in precipitation.

3. 9-yr overview

We first show the seasonal and interannual variation of the key water and energy budgets in the ECMWF model, averaged over the Red–Arkansas River basins, and compare the precipitation with the Higgins et al. observations. In this section we show the 9 yr, 1985–93, at a 5-day resolution. We constructed 5-day averages (or 5-day sums for the hydrology) from the hourly data. For the two leap years (1988 and 1992), day 366 was included with days 361–365.

a. Model hydrology

Figure 2 summarizes the major terms in the (liquid) hydrology for the model analysis from 1985–93 in mm $(5\ \text{days})^{-1}$. The upper and lower curves are the 5-day total rainfall (light solid) and evaporation (dashed). Rainfall is noisy, even as a 5-day basin total. Evaporation shows a clear annual cycle (high in summer), and some interannual variation can be seen, such as low evaporation in 1988, which was a dry summer, and high evaporation in 1989. The solid central curve is the contribution to soil water from nudging. It too has a clear annual cycle, positive in summer and smaller negative in winter, which will be discussed in section 5a. Although it is typically smaller than the rainfall, the net annual contribution from nudging is of order 120 mm, about 15% of the evaporation, and comparable to the annual cycle of soil water (see later).

Figure 3 shows the model soil water balance. The solid curve is the total model soil water for all four soil layers (a total depth of 2.89 m), which falls from 800 mm in 1985 to a low near 650 mm in 1988, and is only partially restored by 1993. The annual range is typically 100 mm, and the interannual range is similar but perhaps somewhat smaller. The dashed curve is the residual recalculated from the separate model terms (with the sign convention that Evap and RunOff are negative) as

$$\text{Resid} = \text{Rain} + \text{Nudging} + \text{SnowMelt} + \text{Evap} + \text{RunOff}. \quad (2)$$

This residual should balance the soil water change, if the model and our nudging calculation were exact. Over 9 yr the residual in Fig. 3 diverges by -40 mm from the total soil water, which amounts to an error of about 5 mm yr^{-1}, out of a typical total nudging of about 120 mm yr^{-1} (the annual precipitation is about 830 mm yr^{-1}). We are uncertain of the source of this error, other than the accumulation of small errors in the nudging calculation.

The annual and interannual range of soil water storage in the ECMWF model is consistent with Roads et al. (1994), who estimated from upper-air and hydrologic measurements that the annual cycle of ''surface water'' storage (the same as our soil water) for the entire Mississippi basin was about 100 mm. In contrast, Roads et al. (1998) in a recent study of the Mississippi basin show

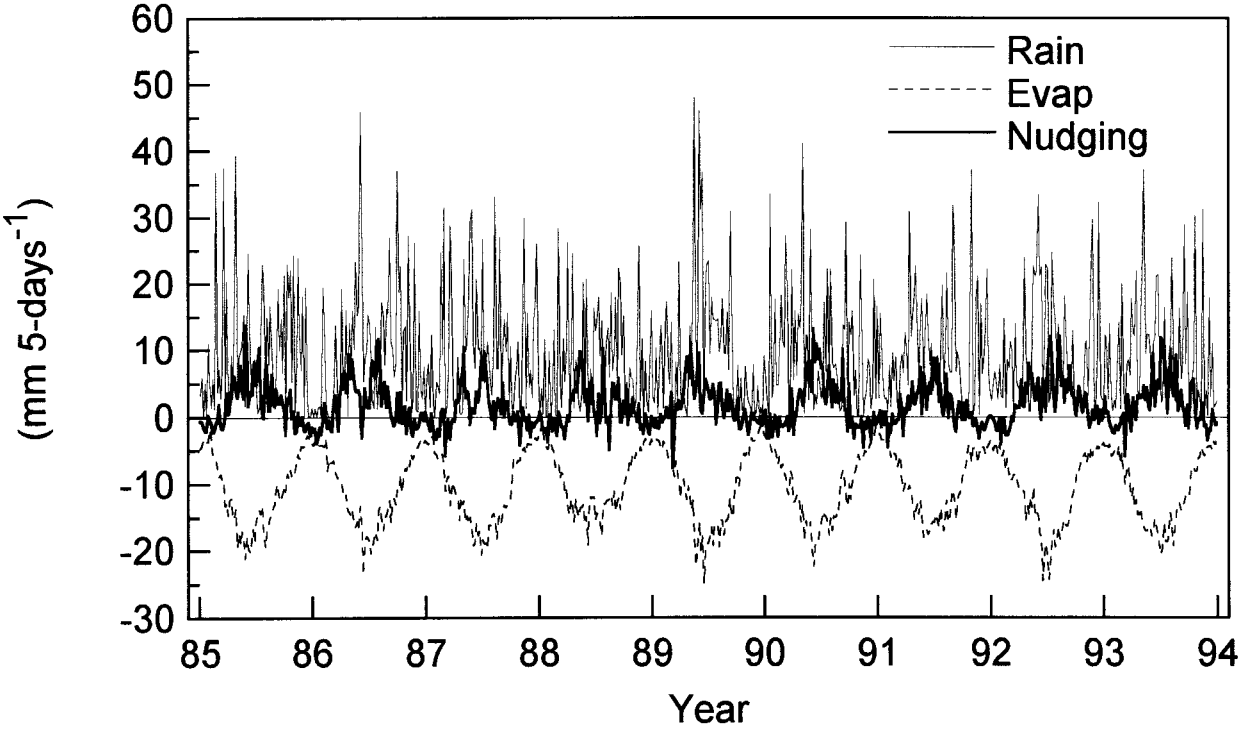

FIG. 2. Five-day average precipitation, nudging, and evaporation (mm) for 1985–93 from model analysis cycle.

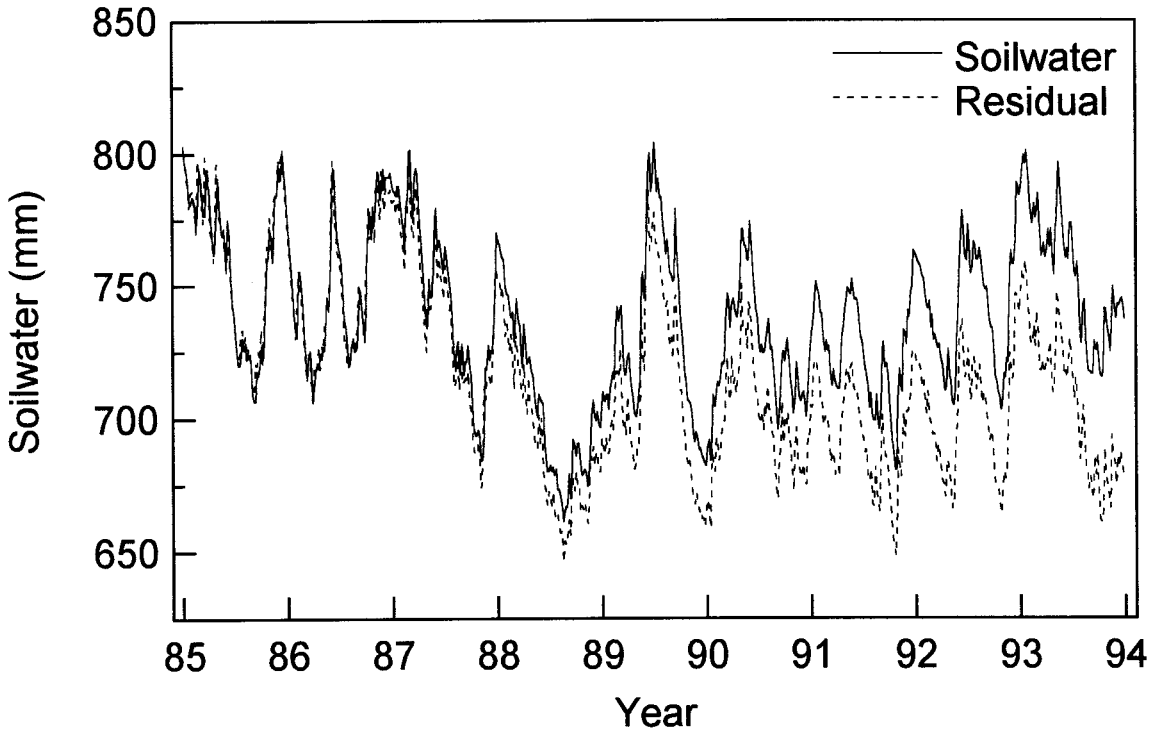

FIG. 3. Change of integrated soil water and residual [Eq. (1)] from 1985–93.

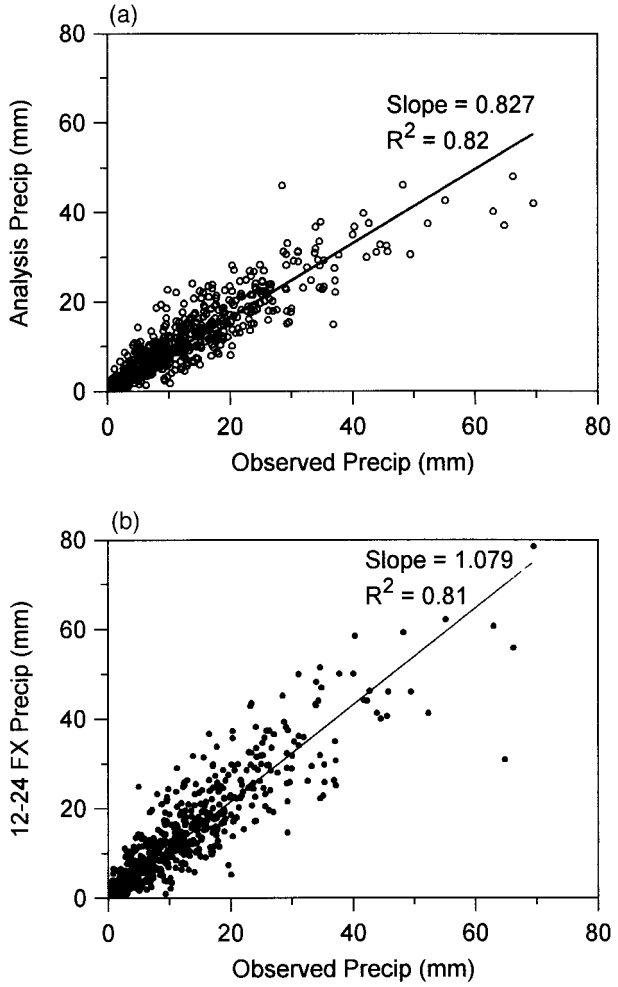

FIG. 4. Scatterplots of 5-day average precipitation for analysis and 12–24-h forecast against observations, showing linear regression lines through origin.

that the NCEP–NCAR reanalysis model has a large annual cycle of surface water of about 300 mm, between a peak of 700 mm and low of 400 mm, and rather little interannual variability. In the same NCEP model running freely in climate mode, surface water falls to about 300 mm in 2 yr, with an annual range of 60–100 mm. In the ECMWF model the nudging of soil water prevents any systematic dry-down, but an apparently realistic annual and interannual variability is preserved. We have no good verification data on the basin scale, but the ECMWF soil water budget is consistent with the upper-air observations driving the reanalysis (although the model has a significant spinup: see later), as well as the mean mixing ratio observations at low levels, which are driving the nudging of soil water.

b. Comparison of 5-day model precipitation with observations

Figures 4a and 4b show scatterplots of the 5-day precipitation for 1985–93 from the analysis (Fig. 4a: open circles) and the 12–24 FX (Fig. 4b: solid circles) against the 5-day observed precipitation [Higgins et al. (1996) data], together with the linear regression lines (with $y = 0$ intercept). We see on the 5-day timescale that the analysis precipitation is less than the observations. The regression line through the origin has a slope of 0.83, but this is influenced by the outliers: for the 9 yr the total analysis precipitation is 0.89 of the observed precipitation. The 12–24 FX precipitation is greater than the observations. Again the regression line has a smaller slope (1.079 as shown) than the ratio of the 12–24 FX precipitation to the observed precipitation (1.15 for the 9 yr). The linear correlation is quite high (R^2 values of 0.81–0.82). Since it is likely that the observations are themselves biased low by about 10% (section 2b), it appears the the 12–24 FX precipitation may have a rather small positive bias, while the analysis precipitation is clearly biased low by about 20%. On this 5-day timescale, the standard deviation of the differences of the model precipitation from the observations is about 5 mm. We consider this correlation of precipitation on the 5-day timescale quite encouraging. However, we will later show that on the diurnal timescale, the model precipitation has a large error.

c. Model thermal balance

Figure 5 shows the nine annual cycles of the thermal balance, again plotted from 5-day average data. The upper curve (solid) is net radiation (RNet) with fluctuations on the 5-day timescale associated with clouds and precipitation in the model. The RNet is small in midwinter. The model ground storage, has a small ± 10 W m^{-2} seasonal variation (not shown). The lower curves are the model latent (LH: light solid) and sensible (SH: dotted) heat fluxes. Here we see the most interannual variability, which is related to rainfall and soil water in summer. In 1988, the driest summer, LH is low and SH is large relative to wetter summers, such as 1986, 1989, or 1992. The SH flux is near zero in midwinter, although it is known that the model has stable BL errors in winter (Viterbo et al. 1997). The LH flux is larger than the SH flux at all times and it is upward even in winter. It is possible that the winter value is too high, because of the lack of a seasonal vegetation cycle in the model. The 9-yr analysis cycle annual averages of RNet, LH, and SH are 97.7, -64.9, and -32.0 W m^{-2}, respectively, giving an annual mean Bowen ratio of 0.49.

However, during this study we found a 7% inconsistency in the surface energy and water budgets. In an earlier model version (Blondin 1991), the surface code used a truncated Taylor expansion of the evaporative flux calculated (earlier in the time step) in the BL part of the code. This approximation, which produces an error in the evaporation of intercepted water, was not reevaluated when the land surface model was updated (Viterbo and Beljaars 1995). A consequence is that the basin average latent heat flux in the surface energy bud-

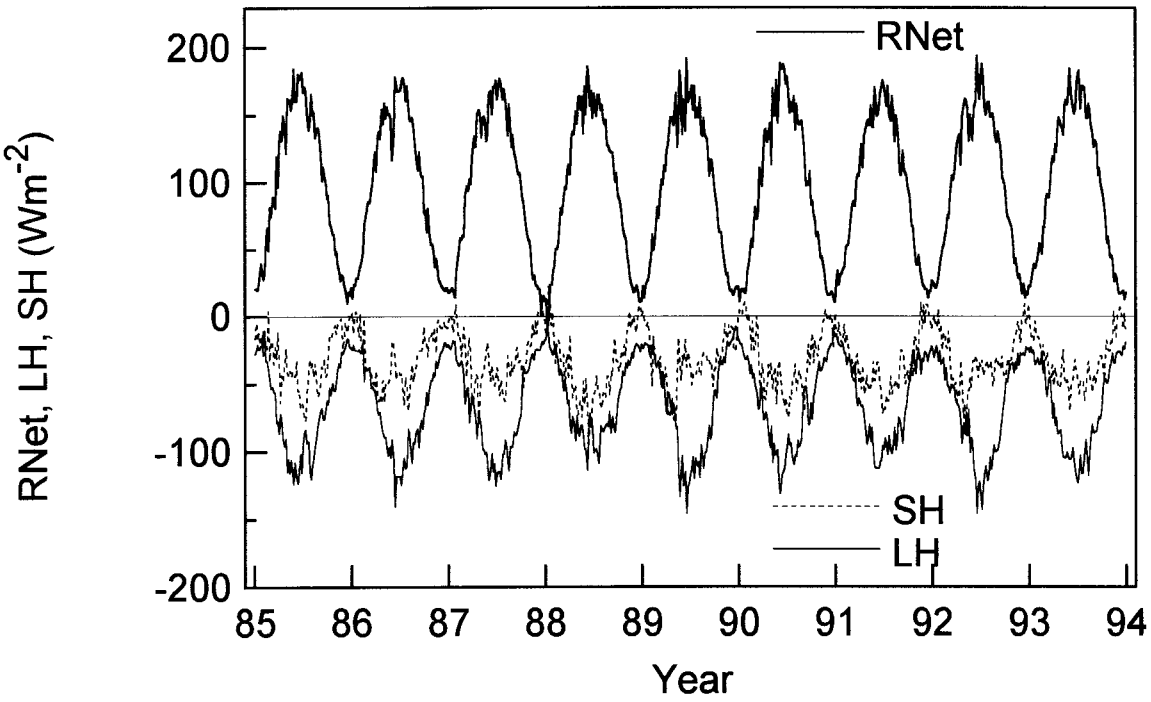

FIG. 5. Five-day average of surface net radiation, and sensible and latent heat for 1985–93 from model analysis cycle.

get, converted to the same units, is 7% higher on average than the liquid evaporation in the subsurface hydrology. This model inconsistency, as well as the nudging of soil water in the model, adds uncertainty to our analysis of the surface water and energy balance.

d. Reanalysis model water balance, 1985–93

Table 2 shows key terms (in mm) in the annual ''liquid water'' budget. The first two columns are the 12–24-h forecast rainfall (the sum of convective and large-scale rain) and the 0–6-h forecast rainfall in the analysis cycle. The next column is the analysis cycle total evaporation (from soil, vegetation, and wet canopy). Evaporation is greater than the analysis rainfall, because the nudging supplies additional soil water (next column), roughly 15% of the total evaporation. The runoff in the model is all deep runoff (9.6% of evaporation). The Δ (soil water) column is the total change of soil water storage during that year. Note the fall in the dry year of 1988, which is partly replenished in the following years. Over the 9 yr, 1985–93, the net change of soil water storage is -68 mm. The last column shows the residual, calculated from Eq. (1), which each year closely balances the change of column soil water. However, in each year there is a small imbalance, which totals -40 mm in 9 yr, as seen in Fig. 3. This could be model error, but is probably the accumulation of small errors in our calculation of the nudging term (of order 5 mm yr^{-1}).

e. Comparison of model with observations, 1985–93

Table 3 compares the total precipitation (which includes snowfall) with observations. The first three col-

TABLE 2. Model liquid hydrology components in mm, 1985–93.

Year	Rain (12–24 FX)	Rain analysis	Evap	Nudging	Runoff	Δ(soil water)	Residual
85	880.6	733.8	−798.8	138.6	−106.5	−29.0	−30.5
86	902.2	728.7	−785.1	136.4	−75.6	11.4	7.0
87	985.2	764.3	−784.4	67.0	−79.3	−16.7	−25.9
88	750.0	616.1	−711.4	75.9	−43.6	−58.5	−60.4
89	934.4	707.3	−760.8	112.7	−87.7	−22.7	−26.4
90	988.7	737.9	−775.4	124.5	−52.4	44.3	38.8
91	984.4	722.3	−718.3	95.0	−81.8	28.8	19.7
92	913.1	702.3	−806.2	180.4	−62.5	21.2	16.1
93	926.6	699.8	−793.6	133.2	−89.2	−47.3	−47.1
Average	918.4	712.5	−770.4	118.2	−75.4		
Sum	8265.2	6412.5	−6933.9	1063.7	678.5	−68.2	−108.6

TABLE 3. Model precipitation, snowfall, and runoff, and observed precipitation and streamflow.

Year	Snowfall (analysis)	Snowfall (12–24 FX)	Snow melt	Precip (analysis)	Precip (12–24 FX)	Precip (Higgins)	Precip (Wood)	Streamflow	Runoff
85	20.0	28.4	2.4	753.9	908.9	836.9	869.9	−173.6	−106.5
86	15.0	23.7	2.5	743.7	926.0	814.3	847.7	−131.1	−75.6
87	35.4	55.2	6.5	799.6	1040.4	861.8	862.2	−146.7	−79.3
88	28.3	41.0	2.6	644.3	791.0	685.2	653.0	−93.3	−43.6
89	18.1	23.8	2.1	725.4	958.2	783.9		−127.1	−87.7
90	22.3	35.7	4.1	760.2	1024.4	925.2		−203.9	−52.4
91	19.3	30.0	2.6	741.6	1014.4	911.2			−81.8
92	19.7	26.8	2.1	722.0	940.0	805.0			−62.5
93	21.5	30.8	2.6	721.3	957.4	819.7			−89.2
Avg	21.2	32.8	3.1	734.7	951.2	827.0	(808.2)	(−146.0)	−75.4

umns relate to the model snow. The model analysis snowfall is less than the 12–24 FX snowfall because of model spinup. The contribution of snowmelt to Eq. (1) is only 3 mm yr^{-1}, small when compared to the mean snowfall of 21 mm yr^{-1} in the analysis [which only contributes to the liquid hydrology through the snowmelt term in (1)]. Adding the snowfall to the rain in Table 2 gives the model precipitation, which can be compared to the observed precipitation in the next two columns from Higgins et al. (1996), and from Woods et al. (1998) (for the years 1985–88).

On an annual basis we see that the observed precipitation lies between the analysis and 12–24 FX precipitation. The last two columns compare the observed stream flow (for 1985–90), and model runoff (repeated from Table 2). We again use the convention that runoff and stream flow are negative. The observed stream flow is roughly double the model runoff. The underestimation of precipitation in the analysis cycle is not a cause of this low runoff. The model has only deep runoff for this basin. The surface runoff is based on a maximum infiltration limit, which is a calculated, following Mahrt and Pan (1982), assuming saturation at the surface and using the model soil water halfway through the first soil layer. Surface runoff occurs when the precipitation rate exceeds this maximum infiltration rate. However, this method is sensitive to the soil vertical discretization, and does not account properly for subgrid-scale variablity in soil water (and the model has only a primitive representation of subgrid-scale convective precipitation), and the result is that there is no surface runoff for this basin.

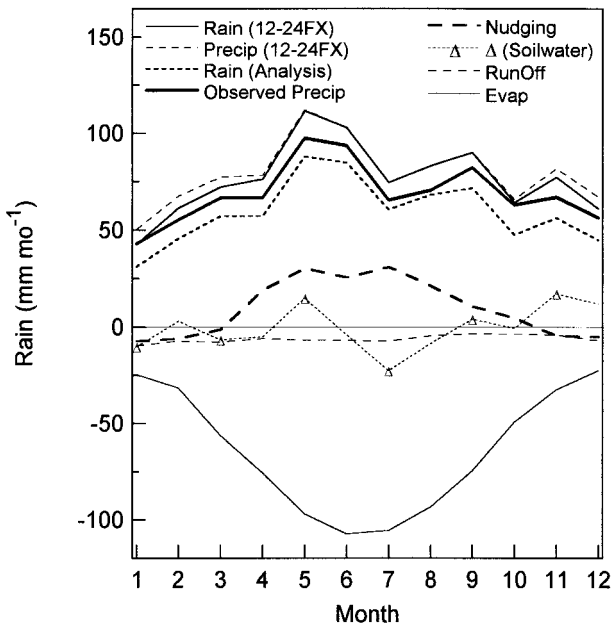

FIG. 6. Nine-year average of model monthly 12–24-h forecast rain, analysis rain, nudging, runoff, evaporation, and soil water change.

4. Monthly hydrological budget: Comparison with observations

In this section we show the monthly mean hydrological budget and compare model precipitation and runoff with basin averaged observations, which we have for 6 yr, 1985–90 for stream flow and 9 yr for precipitation for the Higgins et al (1996) dataset. We will first show the 9-yr average, and then 1988 and 1989 as representative of dry and wet years, as the year-to-year variability is large.

a. 9-yr average

Figure 6 shows the 9-yr average of key terms in the monthly liquid hydrological budget. The units are all mm $month^{-1}$. The upper four curves are rainfall and precipitation, from model and observations. The dotted curve is the analysis rainfall, the heavy solid curve is the observed precipitation, and the highest curves are the 12–24 FX rainfall and total precipitation (to show the small winter snowfall). Rainfall (and total precipitation) peaks in May–June, with a summer minimum in July. The 12–24 FX rain exceeds the rain in the analysis by 35%–40% in midwinter (when large-scale rain dominates) and by only about 22% in midsummer, when convective rain dominates. This model spinup of precipitation will be discussed more in section 5c. In all months the observed precipitation lies between the analysis and 12–24 FX precipitation.

Evaporation in the analysis cycle (the negative light solid curve) peaks in June, and generally exceeds precipitation in midsummer. In sharp contrast to precipitation, the model evaporation has negligible spinup in the warm months, while in winter evaporation has a very small ''spindown,'' which is a maximum of −10% (about 2 mm month^{-1}) in December and January (not shown). The model runoff on this scale is small and rather flat. A significant component of the model budget is the nudging of soil water (heavy dashed line), which is the water added to the soil during the analysis cycle every 6 h based on the short-term forecast error of mixing ratio. It is positive from April to October, about 25 mm month^{-1} in midsummer, as noted in Betts et al. (1998), and somewhat surprisingly it is negative, although small, in winter. Nudging was introduced in the model to compensate for the deficit of precipitation in the analysis cycle. The model spinup of precipitation is there at all times of the year, with a mean value of about 17 mm month^{-1}. This is larger than the (observed − analysis) precipitation difference, which has a mean of 8 mm month^{-1}, although we believe the precipitation observations to be biased about 10% low. On an annual basis, the nudging has a mean of 10 mm month^{-1}, so there is a suggestion that the addition of water by nudging may be compensating for the underestimate of precipitation in the analysis cycle, but only in the annual mean. The annual cycle of nudging will be discussed further in section 5a.

The monthly change of soil water is shown as light dots. The primary recharge of the soil water reservoir is in May and late in the year; while soil water falls in midsummer on average (however, as shown in the next section, there is considerable interannual variability, so this 9-yr mean for soil water changes is not very informative).

b. Monthly hydrologic budget for 1988 and 1989

Individual years show considerable variability from the general pattern of Fig. 6, the 9-yr mean. We show just 2 yr as illustration, Figs. 7a and 7b for 1988 and 1989, dry and wet years, respectively, as representative of extremes. For 1988, we have two sets of precipitation measurements. The upper four curves are the observed precipitation (Higgins, heavy solid, and Wood, light solid), the analysis precipitation (dotted), and the 12–24 FX precipitation. The model spinup in precipitation is visible in all months. However, the relative magnitudes of the observed precipitation and 12–24 FX precipitation in individual months is less clear than in the 9-yr mean in Fig. 6. The two estimates of precipitation differ by 5–10 mm in individual months. In the 4-yr average (1985–88), the Higgins dataset has more precipitation in winter and less in summer (by about 5 mm month^{-1}) than the Wood dataset (not shown).

The year 1988 shows a significant fall of soil water from April to August, and a small recharge in the fall;

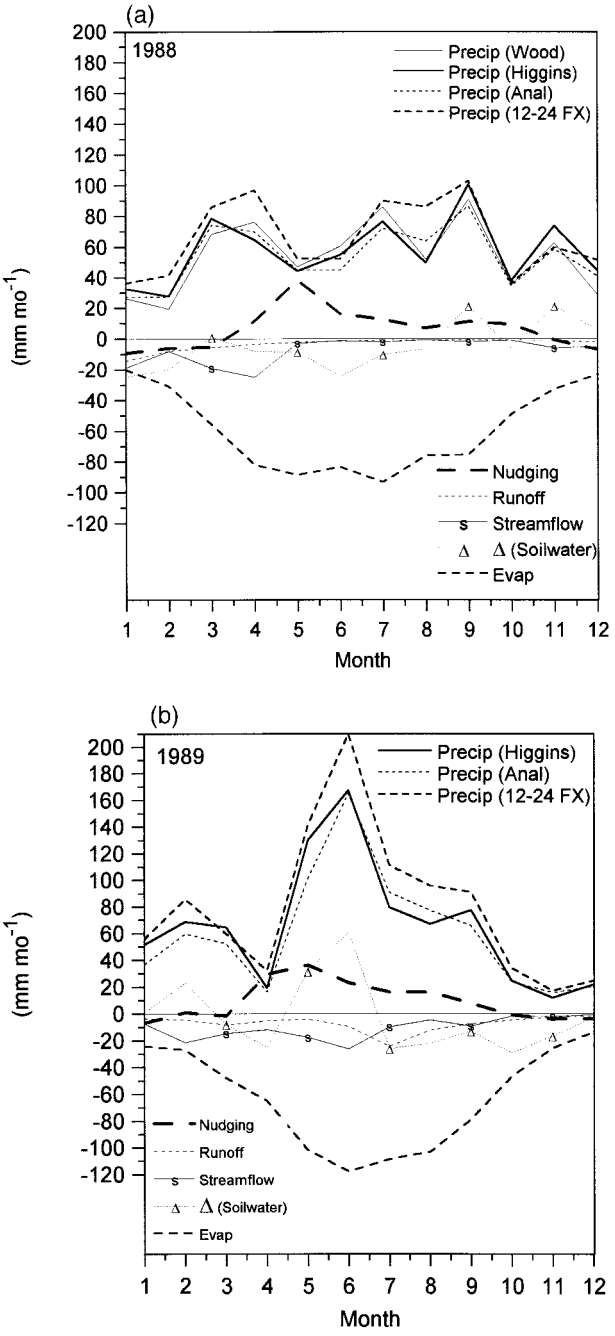

FIG. 7. (a) Monthly precipitation for 1988 from observations, 12–24-h forecast and analysis cycle of model, model nudging, evaporation and runoff, soil water change, and observed stream flow. (b) As in (a) for 1989.

however, the soil water has a net loss during the year (see Table 2). In contrast, in 1989, the large precipitation in May and June significantly recharges the soil water, although low precipitation in the fall means that there is still a net loss for the year. In 1988, both runoff and stream flow are very small from May to October, but the stream flow is larger than the model runoff in spring

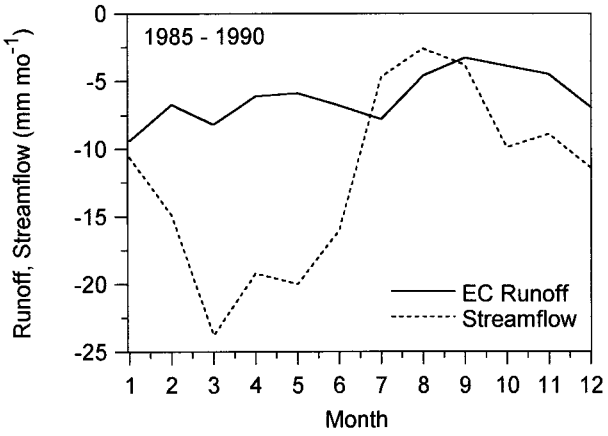

FIG. 8. Comparison of 1985–90 average model runoff and observed streamflow.

and fall. In 1989, the model runoff is small in May and June, despite the high rainfall (as there is no surface runoff); but runoff becomes high in July, when the deepest layer reaches saturation. The observed stream flow has the opposite pattern. This will be discussed more in the next section.

There is significantly less evaporation from May to August in 1988, and the nudging of soil water is also less in the dry year, suggesting that the nudging algorithm may respond to the drier atmospheric conditions. Evaporation is a critical term in the water and energy budgets for which we have only the model estimate: there are no basin-scale measurements of evaporation. So it is important, but difficult, to try to assess its probable absolute and relative year to year accuracy. From the perspective of GCIP this is a key issue, because we must rely on models to give us basin-scale estimates of evaporation. To do this we must first look more closely at the runoff comparison.

c. Comparison of observed and model runoff

Runoff from the ECMWF model is generally very smooth, as it is all ''deep'' runoff, from the layer 4 (100–289 cm). The model has no surface runoff for this basin. Figure 8 shows the 6-yr average for 1985–90 for the monthly averaged model runoff, and the measured stream flow for the whole basin. The model deep runoff does not reflect the spring and fall streamflow peaks, so that on an annual basis, the model runoff is only about half the measured streamflow (see Table 3). This is a significant deficiency in the model. In the real world, the net atmospheric water convergence for this basin (in long-term means) balances precipitation and evaporation, which balance runoff. However, this is not true in the model, as the analysis precipitation is too low (because of the model spinup problem), nudging supplies soil water, trying to get the BL water vapor balance correct, and, in addition, there is a model inconsistency in the surface energy and water balance (section 3c). Koster and Milly (1997) have discussed the close interplay between runoff and evaporation in land surface models driven by fixed atmospheric forcing. However, because the supply of soil water by nudging is larger than the model runoff, and the precipitation, radiation, and other atmospheric forcings are derived interactively during the data assimilation, we cannot directly apply their results to the ECMWF reanalysis.

In the dry year of 1988, both model and measured runoff are less than the average in spring and summer, but again the model deep runoff does not reflect the heavier March–April streamflow (see Fig. 7a). Two examples clearly show the physical difference between the model deep runoff and real streamflow. The small peak for July for the model runoff in Fig. 8 is entirely caused by a runoff of 24 mm for July 1989, shown in Fig. 7b, when the lowest model soil layer reached a prescribed threshold after heavy rain in the preceding two months. The observed streamflow peaked the previous month, and was only 10 mm in July. In contrast, the observed streamflow for May 1990 was 59 mm after prolonged spring rain, but the deep runoff was only 11 mm (not shown), because the lowest model layer did not reach the prescribed threshold where runoff increases rapidly. If the measured streamflow is deconvolved using a hydrograph to approximate the instantaneous average surface runoff, rather than that measured at the mouth of the basin, this smooths the monthly observations a little (not shown), but does not change the overall comparison.

d. Assessment of annual evaporation

We can estimate 6-yr mean basin evaporation for the period 1985–90, for which we have both precipitation and streamflow observations (Table 3) as

$$\begin{aligned}\text{Evap(obs)} &= \text{Precip} - \text{Stream flow} - \Delta(\text{Soil water})\\ &= 818 - 146 + 12 = 684 \text{ mm}, \end{aligned} \quad (3)$$

where we have added a small mean decrease of 12 mm yr^{-1} in soil water, using the model value from Table 2. The mean model evaporation for 1985–90 is

$$\begin{aligned}\text{Evap(model)} &= \text{Evap(liquid)} + \text{Evap(snow)}\\ &= 769 + 10 = 779 \text{ mm}. \end{aligned} \quad (4)$$

Although the model evaporation is higher than the estimate given by (3) by 95 mm, we know that the precipitation measurements are probably low by perhaps 10% or 80 mm. Thus, the model annual evaporation may be at most a few percent high. However, the model has an internal inconsistency of 7% in its evaporation calculation (section 3c), which needs to be corrected before we can truly assess the model evaporation. In an earlier study, Betts et al. (1998) suggested that evaporation might be low in spring and high in fall (and probably also in winter), as the model has no seasonal

cycle of vegetation, so we will look at the seasonal cycle of the nudging in the next section.

5. Discussion of reanalysis model characteristics

In this section we examine some of the reanalysis model characteristics in more detail, specifically the diurnal, 5-day, and seasonal structure of the nudging, the spinup and diurnal cycle of precipitation, and the summer coupling between soil water, soil temperature, and the low-level thermodynamics.

a. Seasonal and diurnal cycle of nudging of soil water

The nudging of soil water in the reanalysis model is an important component of the soil water budget. It has both a marked seasonal and diurnal cycle. The heavy dashed line in Fig. 6 is the 9-yr mean annual cycle of the monthly addition (subtraction) of soil water by nudging. It is positive from April to October and negative in the winter months. Since it is based on the 6-h forecast error in near-surface humidity, this means that the model 6-h forecast is dry (in the 24-h average) relative to the observations from April to October and moist in the cold months. The dry bias in summer is probably related to the shortfall of precipitation in the analysis cycle, which the nudging is replacing. One possible reason for the cold season moist bias is the lack of a seasonal cycle in the vegetation model (Betts et al. 1998), so that evapotranspiration is probably too high in winter. If so, the nudging is trying to reduce this by reducing soil water. This is clearly undesirable in the annual water budget. Another possibility is that the model evaporation scheme is in error at cold temperatures ($<$284 K), but this seems unlikely. A third possibility is that the stable BL errors in the reanalysis model (Viterbo et al. 1997; Betts et al. 1998), which are more significant in winter, are producing too shallow a daytime BL, so that the surface evaporation is trapped in too shallow a layer.

The nudging also has a significant diurnal signal. Figure 9a shows the 9-yr average diurnal cycle of the nudging of the 0–7 cm soil water, SW1 for the ''summer'' months, May–September; the transitional months April and October; and the cold months, November–March. There are values only at the four analysis times. At 1800 UTC (near 1200 LT) the nudging is negative in all three, implying the model 6-h forecast is too moist, while at 0000 (or 2400) UTC (1800 LT) at the end of the daytime heating cycle, the nudging is large and positive in summer, but not in winter. This 0.1% amplitude diurnal cycle in the nudging for the first layer is a model artifact. Fortunately it is smaller than the 0.6% diurnal cycle of soil water, which has a realistic sunset minimum. This diurnal nudging behavior may be related to possible errors in the model diurnal cycle of mixing ratio, since the nudging is related to the lowest model level analysis errors [Eq. (1)]. Figure 9b shows the corresponding 9-yr ''winter'' and summer averages for the four 6-h forecast segments of the model diurnal cycle of mixing ratio, q, (at model level 31, about 30 m above the surface) from each analysis time, marked ''A'' for the summer average and ''a'' for the winter average. During summer (solid curves with left-hand scale), there is a marked late morning peak (1500 UTC) in mixing ratio, followed by a late afternoon minimum, which is not seen in the diurnal cycle of the analysis, the five points marked ''A.'' The nudging is calculated from the difference between the analysis and the 6-h forecast at the same time, so we see that the nudging pattern in Fig. 9a is caused by the low model 6-h q forecast at 0000 and 0600 UTC relative to the analysis and the high model forecast at 1800 UTC. The winter pattern (dashed with right-hand scale) is somewhat similar, except that the model q maximum is later at 1800 UTC, and the afternoon fall of q is very small. The negative nudging at 1800 UTC is larger than the positive nudging at 2400 UTC, so that the negative nudging dominates in the daily sum. For the April and October average (not shown), the morning

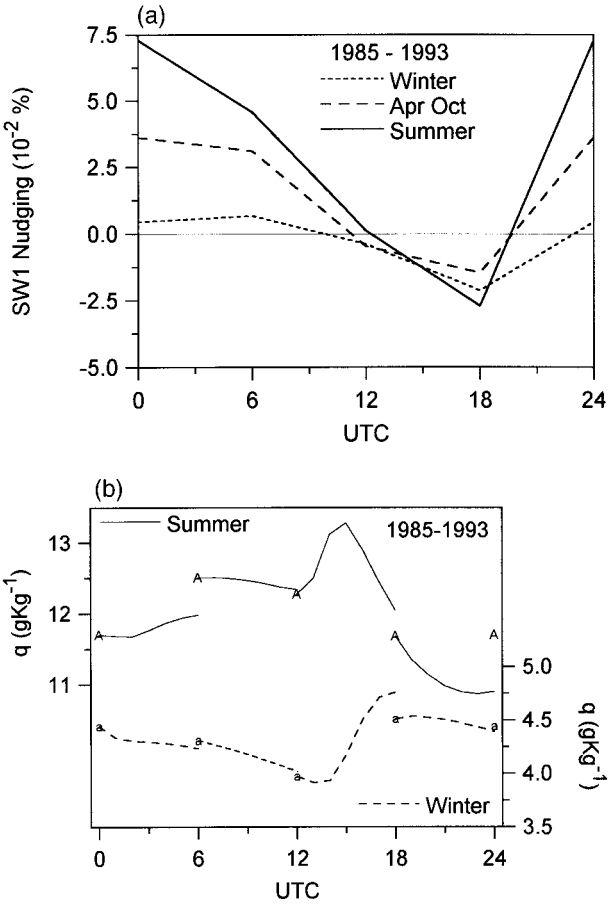

FIG. 9. (a) Average for 1985–93 of diurnal cycle of nudging of 0–7-cm soil water for winter (November–March), April and October, and summer (May–September). (b) Diurnal cycle of lowest model level mixing ratio in analysis cycle for winter and summer averages corresponding to (a).

peak of q is at 1600 UTC, and the nudging is in between. Short-term 24-h forecasts of the model show a similar diurnal pattern (not shown) to Fig. 9b, without of course the discontinuities at the analysis times.

This basin-scale diurnal behavior in summer is very similar to that seen in Betts et al. (1998). In a comparison of the ECMWF reanalysis against the FIFE data, they showed that in summer the model has an erroneous morning maximum and a late afternoon minimum of mixing ratio. These errors appear, in turn, to be related to errors in the model boundary layer depth: too shallow in the morning (following too stable a BL at sunrise), and too deep in the late afternoon. In winter, Fig. 9b shows that with a later sunrise, the morning q maximum is shifted to 1800 UTC, and it has a larger peak than the analysis. If there is relatively more evapotranspiration in the cold season, due to the absence of a seasonal vegetation cycle, and too shallow a boundary layer at sunrise (because of stable BL errors in the model at night), then this would produce too strong a q peak in this model 6-h forecast. In winter, the late afternoon minimum of mixing ratio in the model is much smaller than in summer, so the evening dry bias of the model is much smaller (Fig. 9b). Higher daytime evaporation in the model could again be the reason.

From the perspective of the water budget, the precipitation has a deficit in the analysis cycle at all times of the year, so one might expect the nudging to be positive in all months. If the negative nudging in winter is a response to excessive evaporation, as seems possible, then both the high evaporation and nudging are removing water from the soil. This will reduce the annual cycle of soil water in the model. The model does, of course, have too little runoff, which is largest in the cooler months (Fig. 8). If this were corrected, nudging would have to increase in most months, and more in winter. Our main conclusion is that although the behavior of the nudging is complex, as it interacts with model errors on diurnal and seasonal timescales, it does provide useful information on these other model errors.

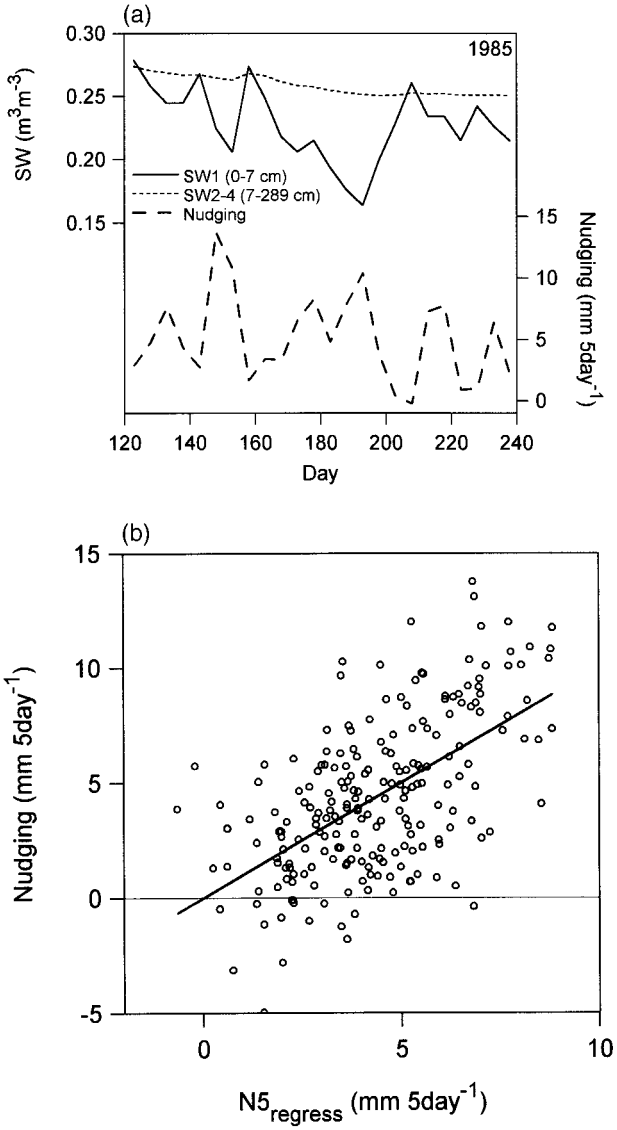

FIG. 10. (a) Shallow and deep soil water (upper curves) and 5-day average nudging during summer, 1985. (b) Scatterplot of nudging against $N5_{regress}$ from (5), together with 1:1 line.

b. Coupling of 5-day nudging to model variables

Figure 10a shows the 5-day nudging and the variations of 0–7-cm layer soil water (SW1) and deep (7–289 cm) soil water (SWD) from May to August 1985. An inverse correlation can be seen in this and other summers: in particular, the nudging falls sharply as SW1 climbs. Soil water climbs when rain exceeds evaporation, and evaporation itself is a function of soil water, primarily through the dependence of evapotranspiration on root zone soil water through a vegetative resistance. There is one extended period in midsummer (days 166–195) of low rainfall (just visible in Fig. 2) when the mean 0–7-cm soil water drops close to the model specified ''permanent wilting point'' of 0.17 $m^3 m^{-3}$ (Viterbo and Beljaars 1995), but the soil water is then recharged by heavy rain. The nudging responds to errors in evaporation as seen by low-level mixing ratio, so as discussed in the previous section the relationships are complex. We therefore used multiple linear regression to explore the dependence of the pentad nudging on soil water (SW1 and SWD), evaporation and rainfall (both in mm), and other variables for the summer months May–August for the 9-yr period, and found

$$\begin{aligned} N5_{regress} = {} & (-16.1 \pm 2.8) - (108 \pm 12)SW1 \\ & + (148 \pm 29)SWD + (0.13 \pm 0.03)RAIN \\ & - (0.37 \pm 0.11)EVAP. \end{aligned} \quad (5)$$

The dependence on 0–7-cm soil water SW1 alone explains only 13.5% of the variance; adding deep soil water SWD increases the explained variance to 29%;

and with evaporation (EVAP) and analysis rainfall (RAIN) included as well, 35% of the variance is explained. The explained variance is not that large, but Fig. 10b, showing the scatterplot of $N5_{regress}$ from Eq. (5) against nudging is suggestive. There appears to be a large seasonal change in the explained variance. If regression coefficients are calculated for individual months (not shown), the explained variance is 59% for the nine Mays, 50% for June, 47% for July, and only 28% for August.

The coefficient of the dependence of $N5_{regress}$ in Eq. (5) on analysis rainfall is only 0.13. Since analysis rainfall is low by 25%, we might expect a higher coefficient, if nudging were primarily making up the deficits in analysis rainfall on the 5-day timescale. We found, in addition, that adding other terms such as the spin up in rainfall (12–24 FX-analysis rainfall) or the deficit of the analysis precipitation from the Higgins observations did not increase the explained variance significantly. The inclusion of evaporation in Eq. (5), which depends on atmospheric variables as well as soil water, increases the explained variance a few percent.

The negative correlation on first layer soil water variations and positive correlation with the deep soil water suggests that the nudging on the 5-day timescale may be compensating for deficiencies in the model. Indeed, because nudging is a response to dry biases in low-level humidity, and therefore implies low evaporation, our provisional conclusion is that the model evapotranspiration may be too dependent on the layer 1 soil water, and insufficiently dependent on the deep soil water. Unfortunately, since we only have an average soil water for the three deeper soil layers 2–4, of which only layers 2 and 3 are in the root zone, we cannot carry this analysis further.

During dry periods in summer, nudging plays a major role in the soil water budget. For example, in the dry month of June 1990, model evaporation remains high near 120 mm, rainfall is small (30 mm), soil water falls about 40 mm, while the nudging supplies about 50 mm of water. It was never intended that nudging should provide such a large percentage of the monthly evaporation. It may be that the model evaporation is too dependent on the soil water in the upper layer, as we commented above. It is also possible that the vegetation can draw on deeper soil water reservoirs than are available in the model. In addition, the model reservoirs may be biased low because of the negative nudging in winter. One might ask whether the model evaporation is too high, but this is unlikely, as the large nudging is being driven by a large dry bias in short-term forecasts of q (albeit with the erroneous diurnal cycle shown in Fig. 9b).

c. *Diurnal cycle of model hydrology spinup and precipitation*

The ECMWF reanalysis model has a significant spinup of the precipitation between the analysis cycle (a 0–6-h forecast) and the 12–24-h forecasts, verifying at the same time. Figure 11 shows four diurnal cycle curves: (the average for 9 yr, 1985–93). The solid pair are for the model large-scale rain and convective rain in the 12–24-h forecasts, and the dotted pair for the corresponding 0–6-h analysis cycle forecasts. From the analysis cycle to the 12–24-h forecast, large-scale rain increases on average by 39%, while the convective rain increases rather less, about 18%. The large-scale snowfall has an average spinup of 48%, but this term is very small for this basin in comparison with liquid precipitation. Convective snowfall is negligible. For the three summer months of June, July, and August, more than 65% of the rain is convective, so that the mean model spinup in summer is only 22%. In the winter most of the rain is large scale, so the spinup is correspondingly larger. The other notable feature of Fig. 11 is that both large-scale and convective rain have maxima near 1800 UTC, close to local noon, which is not the time of the local peak of precipitation in summer.

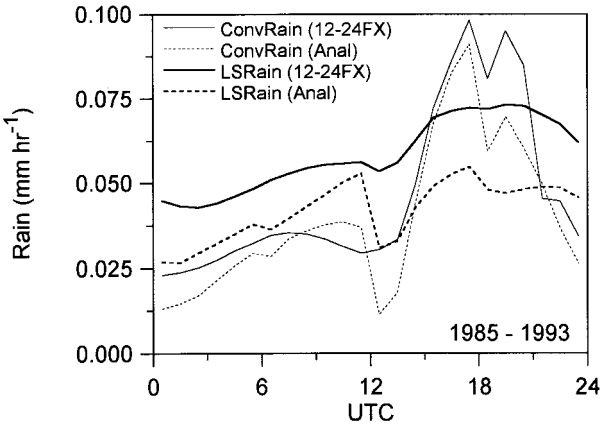

FIG. 11. Spinup of model convective (ConvRain) and large-scale rainfall (LSRain) from analysis cycle to 12–24-h forecast for 1985–93.

Figure 12 shows the average diurnal cycle of total precipitation for the three summer months, June, July, August, for the analysis (dotted), 12–24-h forecast (dashed), and the Higgins precipitation data (solid). The analysis shows the drops in precipitation at the analysis times, which are particularly marked at 1200 and 1800 UTC. Both analysis and 12–24-h forecast have a strong summer precipitation maximum at 1700 UTC, a little before local noon, in strong contrast to the data that has an afternoon to evening maximum, with a secondary peak at local midnight. The Arkansas–Red River basin has, in fact, three geographically distinct rainfall regions (Higgins et al. 1996), which are combined in our basin average. To the west, the diurnal maximum in summer is after sunset, over the Great Plains it is at local midnight, associated with the nocturnal low-level jet from the Gulf of Mexico, while to the east of the basin, there is an afternoon maximum (Higgins et al. 1996). However, it is clear that the diurnal cycle in the ECMWF

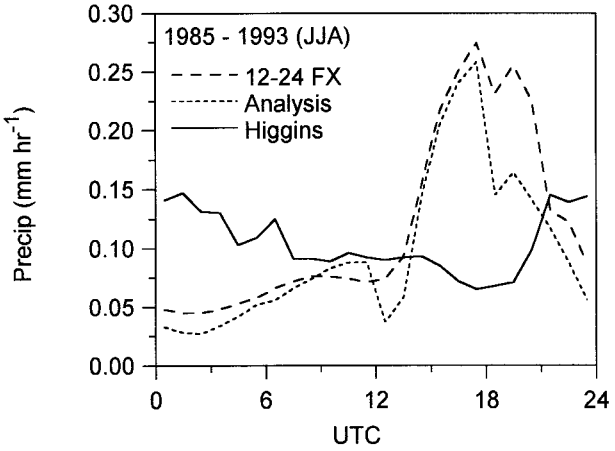

FIG. 12. Comparison of mean diurnal cycle of precipitation for June–August for 1985–93 for analysis, 12–24-h forecast, and observations.

reanalysis model is in error, and has none of these. The reason is still being investigated. One likely contributing cause is the morning peak in mixing ratio at 1500 UTC, shown in Fig. 9b, which we believe to be spurious from Betts et al. (1998), although we have no basin-averaged humidity data for this 9-yr study. The corresponding θ_E peak, a little later at 1600 UTC (not shown), could be directly responsible for the rainfall maximum at 1700 UTC through the convection scheme. The late afternoon minimum in mixing ratio seen in Fig. 9b, may also, at the same time, be suppressing the evening convection. In addition, the model may not be producing the convective mesosystems that are associated with the nocturnal jet. However, despite this error in the diurnal cycle, when we average over 5 days, observed precipitation lies between the analysis precipitation and the 12–24-h forecast precipitation (as shown earlier in Fig. 4).

d. Midsummer coupling between soil water and near-surface thermodynamics

We saw in Fig. 5 that evaporation is considerably lower in years such as 1988 that have less precipitation. In fact, the 5-day average ECMWF data shows a similar coupling in midsummer on the 5-day timescale between soil water, evaporation, and low-level thermodynamics as the FIFE data (Betts and Ball. 1998) show on the diurnal timescale. We define a 5-day mean evaporative fraction as

$$\mathrm{EF} = \mathrm{LH}/(\mathrm{SH} + \mathrm{LH}), \qquad (6)$$

where LH and SH are the 5-day averages of the surface sensible and latent heat fluxes. Figure 13a shows the strong coupling between EF and 0–7-cm soil water, SW1. The data plotted are all the 5-day values (1985–93) for which the 0–7-cm mean soil temperatures are >296 K, representative of the warm months.

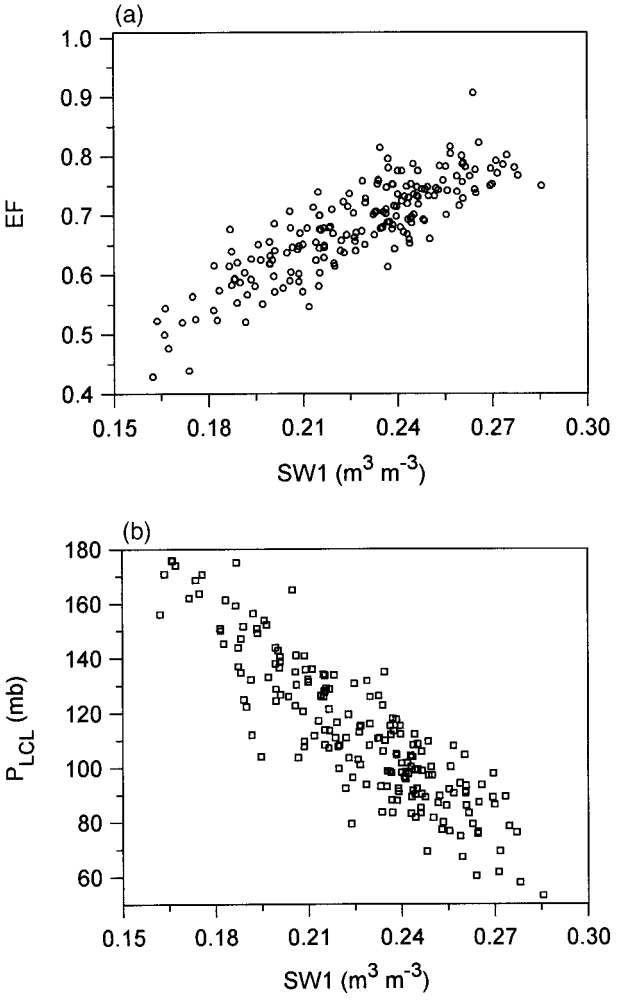

FIG. 13. (a) Scatterplot of 5-day average evaporative fraction over warm soils (0–7-cm layer ST1 >296 K) against 0–7-cm soil water (SW1). (b) As Fig. 13a for pressure height to the lifting condensation level (P_{LCL}).

Figure 13b shows a similar coupling of P_{LCL} (the pressure height of the lifting condensation level) to SW1 for the same data. The model resistance to evaporation between the saturated interior of a ''leaf'' and the surrounding air is dependent on soil water, and this vegetative resistance is therefore one key factor in determining the equilibrium saturation level difference, P_{LCL}, in the saturation pressure budget of the BL (Betts and Ball 1995). We have shown 5-day averages, but the patterns and slopes in Figs. 13a,b are similar (but shifted slightly to higher P_{LCL} and lower EF) if 12-h daytime averages are used instead. Note that the lower limit in Fig. 13b (corresponding to very wet soils) is near the oceanic equilibrium of $P_{LCL} \approx 60$ mb (e.g., Betts and Ridgway 1989). The oceanic surface boundary is saturated, and has no additional resistance to evaporation corresponding to the vegetative resistance over land.

Figures 13a,b are particularly significant because neither of these relationships of EF or P_{LCL} on soil water

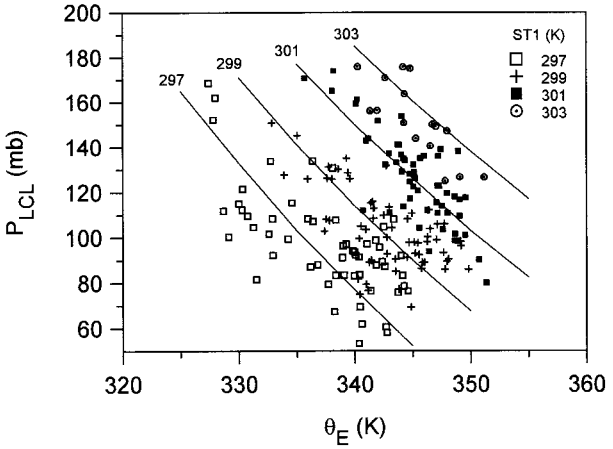

FIG. 14. Scatterplot of P_{LCL} against equivalent potential temperature, θ_E, for 5-day averages in four soil temperature ranges (0–7-cm layer). Labeled lines are the theoretical relationships between P_{LCL} and θ_E at constant temperature

depend strongly on soil temperature at these warm temperatures (not shown). However, the other near-surface thermodynamic variables (θ, q, and θ_E) are strongly coupled to soil temperature (Betts and Ball 1998), as this is coupled to air temperature. Figure 14 is a plot of P_{LCL} against θ_E for (0–7 cm) soil temperatures $>$296 K in 2-K ranges of soil temperature. In each soil temperature range, we see a band from high P_{LCL} and low θ_E (corresponding to low soil water from Fig. 13b) to low P_{LCL} (corresponding to low-mean cloud base) and high θ_E (and high soil water). The plotted lines are simply the relationship between P_{LCL} and θ_E for the constant temperatures, shown as labels. The variation seen in the data, stratified by soil temperature, corresponds to these theoretical lines, because soil and air temperature are well coupled. Because the coupling of P_{LCL} to soil water (Fig. 13b) is independent of soil temperature, at a given soil temperature θ_E increases with increasing soil water and P_{LCL} decreases. In midsummer, soil temperatures plateau not much above 300 K. Since low P_{LCL} and high θ_E favor moist convection, this suggests that the model has the possible summer feedback mechanism between high soil water and more deep moist convection, suggested by Betts and Ball (1995, 1998).

6. Conclusions

We have analyzed the surface energy and water balance in the ECMWF reanalysis model using hourly averages for the Red–Arkansas River basins for the nine available years: 1985–93. The model shows the monthly, seasonal, and interannual variability of precipitation, evaporation, and soil water. The model has a significant spinup in the precipitation between the analysis cycle (based on a 0–6-h forecast), and the 12–24-h forecasts verifying at the same time. The model spinup of large-scale precipitation is 39% on average, while the spinup for convective-scale precipitation is only 18%. Since each contribute about half the precipitation over this basin, the spinup of total precipitation is about 29% on average. Because ''convective'' rainfall exceeds ''large-scale'' rain in summer, while the reverse is true in winter, the model spinup is more in winter than summer. The observations of precipitation lie between the two model estimates, about 12% above the precipitation in the analysis cycle. Since the precipitation observations are if anything biased low, it is clear that the precipitation in the analysis cycle is 20%–25% low, while the 12–24 FX precipitation may be 5% high. The soil water in the model does not dry out, however, because the reanalysis cycle includes nudging of soil water, based on low-level humidity errors every 6 h. Nudging supplies roughly 120 mm yr^{-1} to the soil water budget, and about 15% of the evaporated water. The nudging has a strong seasonal cycle with negative values in winter and positive values (about 25 mm month^{-1}) in summer. The negative values in winter are probably related to two model errors: the lack of a seasonal vegetation cycle, which means winter evapotranspiration is too high, and stable boundary layer errors in winter, which probably cause the winter BL to be too shallow. This would trap the surface evaporation in too shallow a layer, and therefore lead to too high values of model mixing ratio. If the model evapotranspiration is too large in winter, it appears that the nudging of soil water (that is negative in winter) is trying to compensate for this. The removal of soil water by nudging in winter means that more soil water must be added in summer. However, if the model runoff were increased in winter to match the observations, this might increase the winter nudging of soil water (from its present negative value). In addition, the nudging has a marked diurnal cycle linked to the model diurnal cycle of mixing ratio (that probably has a larger diurnal cycle than do observations: see Betts et al. 1998). On the 5-day timescale in summer, the nudging is positively correlated with the (low) analysis rainfall and the deep soil water, and negatively correlated with the first layer soil water and with evaporation. It is possible that the model evapotranspiration may be too dependent on the 0–7-cm soil water, and insufficiently dependent on the deep soil water, but we lack the full resolution of the soil water profile. However, in the course of this study we found a 7% inconsistency in the surface energy and water budgets, dating from an earlier version of the ECMWF model, which did not get reevaluated when the land surface model was updated to cycle 48 (Viterbo and Beljaars 1995). This model inconsistency, as well as the complex interactions of the nudging of soil water with other model errors, adds uncertainty to our analysis of the surface water and energy balance.

The model runoff is all deep runoff; the surface runoff scheme does not appear to be activated in this basin. Consequently, the model runoff does not respond to precipitation in the same way as does observed stream-

flow. The model runoff is generally less than the observed streamflow, except in summer, and on an annual basis, model runoff is about half that observed. The impact of this low runoff on the model hydrological cycle is, however, unclear. The model has no spinup of evaporation in summer and a small spindown in midwinter of about 10%. On an annual basis the model evaporation is only a few percent above a basin average estimate calculated from the observed precipitation and streamflow, if we assume a 10% low bias in the precipitation observations.

We looked at some of the internal characteristics of the model on the 5-day timescale. Evaporative fraction is well correlated with soil water, as would be expected from the vegetation model, which has a soil water sensitive resistance (Viterbo and Beljaars 1995). The pressure height to the lifting condensation level, which is coupled to the vegetative resistance through evaporation, is well correlated to soil water, but not to soil temperature. When we plot the distribution of θ_E against P_{LCL} at warm soil temperatures, we see that even in 5-day averages, high θ_E is correlated with low P_{LCL} (or low cloud base), and high soil water. This is also true if we look just at daytime averaged data. This is the same pattern that was seen by Betts and Ball (1995, 1998) in FIFE data composites on the diurnal timescale. These results suggest that the vegetation model has the internal mechanism for linking soil water to evaporation and convection, through θ_E and P_{LCL}, as suggested by Betts and Ball (1998).

However, on the diurnal timescale, the ECMWF reanalysis model has clear errors, both in the diurnal cycle of mixing ratio, and the diurnal cycle of precipitation. The model has a near-noon precipitation maximum in summer, and does not show the observed late afternoon and evening maximum, nor the secondary nocturnal rainfall maximum, characteristic of the mesoscale systems, which develop over the central part of the basin linked to the nocturnal low-level jet. Whether this is related to errors in the diurnal cycle of q or the inability of the model with T-106 resolution and its convection scheme to develop traveling convective systems is unclear.

Overall the ECMWF reanalysis gives a valuable description of the surface energy and water balance of the Arkansas–Red River basin on timescales longer than the diurnal. This study also suggest several areas where the model needs improvement. Reductions in the model spinup of precipitation are clearly desirable. Although nudging clearly plays an important role in the model hydrology, it appears to control soil water and evaporation in a reasonable way, while trying to compensate for model errors in evaporation and the deficit of analysis precipitation. Improvements in the model diurnal cycle of moisture or boundary layer evolution, a reduction of the precipitation spinup, and a better vegetation seasonal cycle are all likely to reduce the model nudging of soil water. However, increasing the runoff in the model (which has no surface runoff, and a total runoff about half of that observed), as well as correcting the internal model inconsistency in the surface energy and water balance, may increase the nudging.

Acknowledgments. Alan Betts acknowledges support from the National Science Foundation under Grant ATM-9505018, from the NOAA Office of Global Programs under Grant NA76GP0255, and from ECMWF for travel. We are grateful to Wayne Higgins for sending us his hourly precipitation dataset and for helpful advice.

REFERENCES

Abdulla, F. A., D. P. Lettenmaier, E. F. Wood, and J. A. Smith, 1996: Application of a macroscale hydrological model to estimate the water balance of the Arkansas–Red River Basin. *J. Geophys. Res.*, **101,** 7449–7461.

Beljaars, A. C. M., P. Viterbo, M. J. Miller, and A. K. Betts, 1996: The anomalous rainfall over the United States during July 1993: Sensitivity to land surface parameterization and soil moisture anomalies. *Mon. Wea. Rev.,* **124,** 362–383.

Bengtsson, L., and J. Shukla, 1988: Integration of space and in situ observations to study global climate change. *Bull. Amer. Meteor. Soc.,* **69,** 1130–1143.

Betts, A. K., and W. L. Ridgway, 1989: Climatic equilibrium of the atmospheric convective boundary layer over a tropical ocean. *J. Atmos. Sci.,* **46,** 2621–2641.

——, and J. H. Ball, 1995: The FIFE surface diurnal cycle climate. *J. Geophys. Res.,* **100,** 25 679–25 693.

——, and ——, 1998: FIFE surface climate and site-average dataset 1987–89. *J. Atmos Sci.,* **55,** 1091–1108.

——, ——, and A. C. M. Beljaars, 1993: Comparison between the land surface response of the European Centre model and the FIFE-1987 data. *Quart. J. Roy. Meteor. Soc.,* **119,** 975–1001.

——, P. Viterbo, and A. C. M. Beljaars, 1998: Comparison of the land surface interaction in the ECMWF reanalysis model with the 1987 FIFE data. *Mon. Wea. Rev.,* **126,** 186–198.

Blondin, C., 1991: Parameterization of land surface processes in numerical weather prediction. *Land Surface Evaporation: Measurement and Parameterization,* T. J. Schmugge and J. C. André, Eds., Springer, 31–54.

Gibson, J. K., P. Kallberg, S. Uppala, A. Hernandez, A. Nomura, and E. Serrano, 1997: *ERA Description.* ECWMF Reanalysis Project Report Series, Vol. 1, ECMWF, 72 pp.

Groisman, P. Ya., and D. R. Legates, 1994: The accuracy of Unit ed States precipitation data. *Bull. Amer. Meteor. Soc.,* **75,** 215–227.

Higgins, R. W., J. E. Janowiak, and Y.-P. Yao, 1996: A gridded precipitation database for the United States (1963–93). *NCEP/Climate Prediction Center Atlas 1,* 47 pp. [Available from Climate Prediction Center, NCEP, NWS, Camp Springs, MD 20746.]

Koster R., and P. Milly, 1997: The interplay between transpiration and runoff formulations in land surface schemes used with atmospheric models. *J. Climate,* **10,** 1578–1591.

Mahrt, L., and H.-L. Pan, 1982: A two-layer model of soil hydrology. *Bound-Layer Meteor.,* **29,** 1–20.

——, S.-C. Chen, A. K. Guetter, and K. P. Georgakakos, 1994: Large-scale hydrologic aspects of the United States hydrologic cycle. *Bull. Amer. Meteor. Soc.,* **75,** 1589–1610.

Roads, J. O., S.-C. Chen, M. Kanimitsu, and H. Juang, 1998: Surface water characteristics in the NCEP global spectral model and reanalysis. *J. Geophys. Res.,* in press.

Seaber, P. R., F. P. Kapinos, and G. L. Knapp, 1987: Hydrologic

unit maps. U.S. Geological Survey Water-Supply Paper 2294, 64 pp. + map. [Available from USGS, Federal Center, Box 25425, Denver, CO 80225.]

Viterbo, P., and A. C. M. Beljaars, 1995: A new land surface parameterization scheme in the ECMWF model and its validation, *J. Climate,* **8,** 2716–2748.

——, ——, I.-F. Mahfouf, and J. Teixeira, 1997: The role of soil water freezing in the interaction of the surface with the stable boundary layer. Internal ECMWF Memo., 17 pp. [Available from ECMWF, Shinfield Park, Reading RG2 9AX, United Kingdom.]

Wood, E. F., and Coauthors, 1998: The project for intercomparison of land surface parameterization schemes. (PILPS) Phase-2(c) Red-Arkansas River Experiment: 1. Experiment description and summary intercomparisons. *J. Global Planet. Change,* in press.